Z. Phys. C – Particles and Fields 49, 129–139 (1991)

Zeitschrift für Physik C Particles and Fields

Mirror fermion production in ep collisions

F. Csikor

Deutsches Elektronen-Synchrotron DESY, W-2000 Hamburg, Federal Republic of Germany and
Institute for Theoretical Physics, Eötvös University, H-1088 Budapest, Hungary*

Received 25 June 1990

Abstract. The phenomenology of mirror fermions is studied in a model with three heavy mirror fermion families. The tree unitarity bounds on the mirror masses are determined. The production cross-sections and decay characteristics of mirror fermions are calculated in high energy electron-proton collisions. For mirror mixing angles of the order of the present upper limits mirror fermion production at HERA ($\sqrt{s}=314$ GeV) is observable up to masses near 200 GeV. For a possible HERA upgrade ($\sqrt{s}=566$ GeV) this limit goes up to about 350 GeV and an ep collider in the LEP tunnel ($\sqrt{s}=1.4$ TeV) could cover the range below 500 GeV.

1 Introduction

The standard model of electroweak interactions is a highly successful theory. There is no single experimental result which would clearly contradict it. In fact even the necessity of taking into account the one loop corrections is clearly established. Nevertheless from the theoretical point of view the standard model is incomplete, therefore great efforts have been made to study 'beyond the standard model' theories. Such theories very often contain fermions, whose chirality properties are opposite to those of the ordinary fermions, i.e. the right handed components form weak SU(2) doublets, while the left handed are singlets. Such fermions are called mirror fermions. E.g. a possible way of left-right symmetry restoration at high energies is the doubling of the light fermion spectrum by mirror partners at the scale of the electroweak symmetry breaking [1]. Mirror pairs can easily be accomodated in other extensions of the minimal standard model as well (see for instance, the references [2–6] and the review [7]). Moreover, the non-perturbative lattice formulation of chiral gauge theories has difficulties to avoid the mirror doubling of the physical fermion spectrum. The root of these difficulties lies in the fermion doubling phenomenon in lattice regularization [8], implying the presence of mirror partners in the theory with finite cut-off. The mirror partners can also appear dynamically at strong bare Yukawa-couplings, as it was shown in a prototype model using the hopping parameter expansion [9]. In the continuum limit (i.e. at large cut-off) the mirror fermions can become heavy, but at present it is not known whether they can or can not be completely removed from the physical spectrum [10, 11].

Depending on the choice of bare parameters, a non-perturbative formulation of quantum field theories can describe qualitatively different physical situations. A simple example is that the scalar Higgs-sector has two phases: the *symmetric phase* where the O(4)-symmetry of the scalar fields is explicitly realized and the phase with spontaneous symmetry breaking where the non-zero vacuum expectation value of the field breaks the symmetry. In the presence of Yukawa-couplings between the Higgs-field and the fermions the phase structure of the theory is presumably more rich. The hopping parameter expansion at strong bare Yukawa-coupling shows [9, 12, 13] that there is a symmetric phase with degenerate massive mirror fermion pairs. A non-zero scalar vacuum expectation value transforms this explicitly mirror symmetric phase into a phase with *spontaneously broken mirror symmetry* where the mirror partners have different masses and are mixed with each other and with the ordinary fermions. At weak bare Yukawa-coupling there might be other phases without mirror fermions in the physical spectrum, where the mirror asymmetric perturbation theory with decoupled mirror partners [14] can be applied. Even if there were spontaneously broken phases with and without mirror fermions, the question whether nature is in one or in the other phase cannot be answered without an input from experiment.

The presently known phenomenology seems to suggest the absence of mirror doubling, since no effects of the mirror partners of the known fermion families are observed. Nevertheless, in the phase with spontaneously broken mirror symmetry the natural scale of the mirror

* Permanent address

fermion masses is the scale of the vacuum expectation value (i.e. a few hundred GeV) and there are possible mixing schemes with three heavy mirror fermion families which agree with all known experiments [1]. The experimental limits on the mirror fermion admixture in the light fermions are, of course, strongest for the first family. They can be inferred from the simultaneous fits of the present data as done in [15]. To discuss the phenomenology of mirror fermions whe shall use the model of [1]. (The "hermitian mirror fermion model" in [15] corresponds to the model in [1], therefore the mixing angle bounds are known in this case.)

In e^+e^- annihilation (at LEP and SLC) sufficiently light mirror fermions could be pair produced via large couplings proportional to the cosines of the (small) mixing angles. If there is a substantial mixing of the order of the upper limits in [15], single mirror fermions can be produced on the Z-peak by the mixing practically up to a mass of M_Z. The general aspects of phenomenology of mirror fermion production at e^+e^- colliders have been worked out in [16]. Though a dedicated search at LEP has not been performed yet, it seems improbable that mirror fermions lie in this energy range. Therefore, in the present paper we shall concentrate on the mass range above 90 GeV.

The paper is organized as follows. For the reader's convenience in Sect. 2 we review briefly the model of [1]. In Sect. 3 we establish the bounds on mirror fermion masses, which follow from imposing the tree unitarity condition. The cross-section formulae of mirror fermion production in ep collisions are presented in Sect. 4, together with a numerical evaluation. Mirror decay and the final states of mirror production in ep collisions are studied in Sect. 5. Some conclusions are collected in the summary. Mirror lepton production in ep collisions has been previously studied in [17], while [18] already reported a small part of the results for mirror quark production. Some of the results of these papers will be repeated here for the reader's convenience.

2 The hermitian mirror fermion model

To establish notation and for convenience we review here briefly the hermitian mirror fermion model of [1]. This is an extension of the standard $SU(2)_L \otimes U(1)_Y$ model of electroweak interactions. The basic symmetry and the symmetry breaking are the same, while additional fermions, with opposite chirality properties, the mirror fermions are added. The original fields in the Lagrangean are denoted by ψ^{ACK} for the ordinary fermions, and by χ^{ACK} for the mirror partners. $A=1, 2$ are weak $SU(2)$ indices, $C=l, q$ stands for leptons and quarks resp., while $K=1, 2, 3$ is the family index. For each fermion species we have the $6\otimes 6$ mass matrix specifying the mixing pattern. In the $3\otimes 3$ block matrix notation it reads:

$$\begin{pmatrix} \mu_\psi^{AC} & \mu_{\psi\chi}^{C} \\ \mu_{\psi\chi}^{C} & \mu_\chi^{AC} \end{pmatrix} \tag{1}$$

where $\mu_{\psi\chi}^C$ is proportional to the unit matrix and both the hermitian μ_ψ^{AC} and μ_χ^{AC} can be diagonalized by the same 3×3 unitary matrix F_{AC}. It is important that the off diagonal $\mu_{\psi\chi}^C$ is assumed to be independent of the weak $SU(2)$ index. Thus all the 3×3 matrices in (1) are diagonalized by the unitary matrix

$$\begin{pmatrix} F_{AC} & 0 \\ 0 & F_{AC} \end{pmatrix}. \tag{2}$$

The 3×3 Kobayashi-Maskawa matrix is given for both ordinary and mirror fermions by

$$M_{CK_1K_2} \equiv \sum_K F^{-1}_{2C,K_1K} F_{1C,KK_2}. \tag{3}$$

The complete diagonalization of the mass matrix is achieved by the fields

$$\begin{aligned} \zeta^{ACK_1} &= \sum_K F^{-1}_{AC,K_1K}(\cos\alpha_{ACK_1}\psi^{ACK} - \sin\alpha_{ACK_1}\chi^{ACK}), \\ \eta^{ACK_1} &= \sum_K F^{-1}_{AC,K_1K}(\sin\alpha_{ACK_1}\psi^{ACK} + \cos\alpha_{ACK_1}\chi^{ACK}), \end{aligned} \tag{4}$$

where the angles α_{ACK} express the mixing of ordinary and mirror fermions. They are of course expressible with the parameters of the original mass matrix (1).

The electroweak interaction of the fermions can be written as

$$\begin{aligned} &g[J_-(x)_\mu W^+(x)^\mu + J_+(x)_\mu W^-(x)^\mu] + eJ_{em}(x)_\mu A(x)^\mu \\ &+\sqrt{(g^2+g'^2)}[\sin^2\Theta_W J_{em}(x)_\mu - J_0(x)_\mu] Z(x)^\mu. \end{aligned} \tag{5}$$

The vector bosons fields are in the usual notation; Θ_W is the Weinberg angle with $\tan\Theta_W = g'/g$ and the electromagnetic coupling is $e=g\sin\Theta_W$. The electromagnetic current is vector-like and it is diagonal in the fermion fields. The chiral weak currents $J_a (a=+, -, 0)$ are given by

$$J_a(x)_\mu = \bar{\zeta}(x)\Gamma^a_{\zeta\zeta,\mu}\zeta(x) + \bar{\zeta}(x)\Gamma^a_{\zeta\eta,\mu}\eta(x) + \ldots \tag{6}$$

The matrices Γ^a are given by

$$\begin{aligned} \Gamma^{+C,K_1K_2}_{\zeta\zeta,\mu} &= \frac{\tau^+}{\sqrt{8}} M^+_{C,K_1K_2} \\ &\cdot[\gamma_\mu\cos(\alpha_{1CK_1} - \alpha_{2CK_2}) + \gamma_\mu\gamma_5\cos(\alpha_{1CK_1} + \alpha_{2CK_2})], \\ \Gamma^{+C,K_1K_2}_{\zeta\eta,\mu} &= \frac{\tau^+}{\sqrt{8}} M^+_{C,K_1K_2} \\ &\cdot[\gamma_\mu\sin(\alpha_{2CK_2} - \alpha_{1CK_1}) + \gamma_\mu\gamma_5\sin(\alpha_{2CK_2} + \alpha_{1CK_1})], \\ \Gamma^{+C,K_1K_2}_{\eta\zeta,\mu} &= \frac{\tau^+}{\sqrt{8}} M^+_{C,K_1K_2} \\ &\cdot[\gamma_\mu\sin(\alpha_{1CK_1} - \alpha_{2CK_2}) + \gamma_\mu\gamma_5\sin(\alpha_{1CK_1} + \alpha_{2CK_2})], \\ \Gamma^{+C,K_1K_2}_{\eta\eta,\mu} &= \frac{\tau^+}{\sqrt{8}} M^+_{C,K_1K_2} \\ &\cdot[\gamma_\mu\cos(\alpha_{2CK_2} - \alpha_{1CK_1}) - \gamma_\mu\gamma_5\cos(\alpha_{2CK_2} + \alpha_{1CK_1})], \end{aligned} \tag{7}$$

with $\tau^{\pm} \equiv (\tau_1 \pm i\tau_2)/2$. Γ^- is obtained from (7) by $\tau^+ \to \tau^-$, $M^+ \to M^-$ *and* $(A=1) \leftrightarrow (A=2)$. Γ^0 is diagonal in the SU(2) index A and in the family index K:

$$\Gamma^{0,ACK}_{\zeta\zeta,\mu} = \frac{\tau_{3,AA}}{4}[\gamma_\mu + \gamma_\mu\gamma_5 \cos(2\alpha_{ACK})],$$

$$\Gamma^{0,ACK}_{\eta\eta,\mu} = \frac{\tau_{3,AA}}{4}[\gamma_\mu - \gamma_\mu\gamma_5 \cos(2\alpha_{ACK})],$$

$$\Gamma^{0,ACK}_{\zeta\eta,\mu} = \Gamma^{0,ACK}_{\eta\zeta,\mu} = \frac{\tau_{3,AA}}{4}\gamma_\mu\gamma_5 \sin(2\alpha_{ACK})]. \tag{8}$$

The last equations shows that at the tree level there are no flavour changing neutral currents, moreover in the neutral current ordinary fermion – mirror fermion mixing occurs only in the axial-vector part. Putting the mixing angles to zero in (7), (8) we observe the $V \mp A$ structure for ordinary and mirror fermions respectively.

The bounds on the mixing angles obtained in [15] are as follows:

$$\sin^2\alpha_{\nu_e} \leqq 0.05; \quad \sin^2\alpha_{\nu_\mu} \leqq 0.03; \quad \sin^2\alpha_e \leqq 0.03$$
$$\sin^2\alpha_\mu \leqq 0.025; \quad \sin^2\alpha_u \leqq 0.03; \quad \sin^2\alpha_d \leqq 0.05. \tag{9}$$

3 Bounds on the mirror fermion masses from the tree unitarity approach

In this section we present the scattering amplitudes of some processes involving mirror fermions in the tree approximation. Applying partial wave unitarity in the spirit of [19], we get bounds on the Yukawa couplings, i.e. eventually on the mirror masses. The tree unitarity bound gives the value of the Yukawa coupling where the interaction becomes strong. This can also be an absolute upper bound, if strong interaction is not possible as for instance in pure Φ^4 theories [10]. The bounds are obtained at high energies (i.e. energies much higher than all the masses involved), therefore we present the amplitudes only in this limiting case. For simplicity the small mirror mixing angles are set equal to zero.

The amplitudes for processes $F_A(p_1, \lambda_1)\bar{F}_A(p_2, \lambda_2) \to F_B(p_3, \lambda_3)\bar{F}_B(p_4, \lambda_4)$, where F denotes mirror fermions, A, B are SU(2) indices, p_i, λ_i $(i=1, 2, 3, 4)$ are momenta and helicities, are given by

I. For $A=B$

- s channel Higgs exchange:

$$\sqrt{2}\, G_F m_A m_B \lambda_1 \lambda_3 \delta_{\lambda_1,\lambda_2}\delta_{\lambda_3,\lambda_4}$$

- s channel Z^0 exchange:

$$\sqrt{2}\, G_F m_A m_B \delta_{\lambda_1,\lambda_2}\delta_{\lambda_3,\lambda_4}$$

- t channel Higgs exchange:

$$-2\sqrt{2}\, G_F m_A^2 \frac{\sin^2(\theta/2)}{1-\cos\theta}\lambda_1\lambda_2\delta_{\lambda_1,-\lambda_3}\delta_{\lambda_2,-\lambda_4}$$

- t channel Z^0 exchange:

$$2\sqrt{2}\, G_F m_A^2 \frac{\sin^2(\theta/2)}{1-\cos\theta}\delta_{\lambda_1,-\lambda_3}\delta_{\lambda_2,-\lambda_4}. \tag{10}$$

The s channel exchange formulae hold also, when F_A, F_B are fermions of different colour or family, but have the same SU(2) quantum numbers, while the t channel exchange amplitudes are vanishing. (In this case the masses m_A, m_B may be different.)

II. For $A=1$, $B=2$ (i.e. $A \neq B$)

- s channel Higgs exchange:

$$\sqrt{2}\, G_F m_A m_B \lambda_1 \lambda_3 \delta_{\lambda_1,\lambda_2}\delta_{\lambda_3,\lambda_4}$$

- s channel Z^0 exchange:

$$-\sqrt{2}\, G_F m_A m_B \delta_{\lambda_1,\lambda_2}\delta_{\lambda_3,\lambda_4}$$

- t channel W exchange:

$$\sqrt{2}\, G_F \frac{\sin^2(\theta/2)}{1-\cos\theta}[-\lambda_1(m_1-m_2)+(m_1+m_2)]$$
$$\cdot[\lambda_2(m_1-m_2)+(m_1+m_2)]\,\delta_{\lambda_1,-\lambda_3}\delta_{\lambda_2,-\lambda_4}. \tag{11}$$

In all the amplitudes above and below θ means the c.m. scattering angle. Comparing with the results for ordinary fermion scattering, we see that in case I there is no change at all, while in case II the masses enter in a different way.

The nonzero scattering amplitudes for producing longitudinal vector bosons or Higgs bosons at high energy are as follows.

III.

$$F_1(p_1, \lambda_1)\bar{F}_1(p_2, \lambda_2) \to W^+ W^-$$
$$\lambda_1 = -1, \lambda_2 = 1 \qquad -2\sqrt{2}\, G_F m_1^2 \tan\left(\frac{\theta}{2}\right)$$
$$\lambda_1 = 1, \lambda_2 = -1 \qquad 2\sqrt{2}\, G_F m_2^2 \tan\left(\frac{\theta}{2}\right)$$
$$F_2(p_1, \lambda_1)\bar{F}_2(p_2, \lambda_2) \to W^- W^+$$
$$\lambda_1 = -1, \lambda_2 = 1 \qquad -2\sqrt{2}\, G_F m_2^2 \tan\left(\frac{\theta}{2}\right)$$
$$\lambda_1 = 1, \lambda_2 = -1 \qquad 2\sqrt{2}\, G_F m_1^2 \tan\left(\frac{\theta}{2}\right).$$

IV.

$$F_A(p_1, \lambda_1)\bar{F}_A(p_2, \lambda_2) \to HH$$
$$\lambda_1 = -1, \lambda_2 = 1 \qquad -2\sqrt{2}\, G_F m_A^2 \cot\theta$$
$$\lambda_1 = 1, \lambda_2 = -1 \qquad 2\sqrt{2}\, G_F m_A^2 \cot\theta$$

V.

$$F_A(p_1, \lambda_1)\bar{F}_A(p_2, \lambda_2) \to Z^0 Z^0$$
$$\lambda_1 = -1, \lambda_2 = 1 \qquad 2\sqrt{2}\, G_F m_A^2 \cot\theta$$
$$\lambda_1 = 1, \lambda_2 = -1 \qquad -2\sqrt{2}\, G_F m_A^2 \cot\theta$$

VI.

$$F_A(p_1,\lambda_1)\bar{F}_A(p_2,\lambda_2)\to Z^0 H$$

$$\lambda_1=-1,\lambda_2=1 \quad 2\sqrt{2}\,G_F m_A^2\,\tau_{3,AA}(\sin\theta)^{-1}$$

$$\lambda_1=1,\lambda_2=-1 \quad 2\sqrt{2}\,G_F m_A^2\,\tau_{3,AA}(\sin\theta)^{-1}. \tag{12}$$

The amplitudes may be expanded into a partial wave series. Since the partial wave amplitudes a_j satisfy [20]

$$|\mathrm{Re}(a_j)|\leqq\tfrac{1}{2} \tag{13}$$

one gets upper bounds for the Yukawa couplings/masses from the various processes. Every single process gives a bound, however, considering a whole set of coupled channels, condition (13) applies for the largest eigenvalue of the partial wave amplitude matrix as well. Thus in the coupled channel case one may obtain improved bounds. The diagonalization of the matrices is complicated in general. In [19] the special cases considered were:

i) All masses except for a single one equal to zero,
ii) All masses equal.

In our case only the second possibility seems to be sensible. We present the bounds obtained separately for leptone and quarks.

Leptons

The single channel bound for leptons from the $j=0$ amplitudes from processes I is:

$$m_A^2\leqq\frac{2\sqrt{2}\pi}{G_F}=(848.53)^2\ \mathrm{GeV}^2. \tag{14}$$

The process I $j=0$ amplitudes for three degenerate families yield:

$$m_A^2\equiv m^2\leqq\frac{2\sqrt{2}\pi}{G_F}\frac{1}{5}=(388.9)^2\ \mathrm{GeV}^2. \tag{15}$$

The coupled channel problem of the $j=1$ amplitudes of processes I–VI yields for a single degenerate family:

$$m_A^2\equiv m^2\leqq\frac{\sqrt{2}\pi}{G_F}=(617.18)^2\ \mathrm{GeV}^2. \tag{16}$$

The same for three degenerate families results in:

$$m_A^2\equiv m^2\leqq\frac{\sqrt{2}\pi}{G_F}\frac{2}{3}=(503.93)^2\ \mathrm{GeV}^2. \tag{17}$$

Quarks

The single channel bound for quarks from the $j=0$ amplitudes from processes I is:

$$m_A^2\leqq\frac{2\sqrt{2}\pi}{G_F}=(848.53)^2\ \mathrm{GeV}^2. \tag{18}$$

The process I $j=0$ amplitudes for a single flavour, three colour quark yield:

$$m_A^2\leqq\frac{2\sqrt{2}\pi}{G_F}\frac{1}{5}=(388.9)^2\ \mathrm{GeV}^2. \tag{19}$$

Process I $j=0$ amplitudes for three degenerate families of quarks give the bound:

$$m_A^2\equiv m^2\leqq\frac{2\sqrt{2}\pi}{G_F}\frac{1}{17}=(211.0)^2\ \mathrm{GeV}^2. \tag{20}$$

The coupled channel problem of the $j=1$ amplitudes of processes I–VI yields for a single coloured degenerate family:

$$m_A^2\equiv m^2\leqq\frac{2\sqrt{2}\pi}{G_F}\frac{1}{3}=(503.93)^2\ \mathrm{GeV}^2. \tag{21}$$

The same for three degenerate families results in:

$$m_A^2\equiv m^2\leqq\frac{\sqrt{2}\pi}{G_F}\frac{1}{2.386}=(399.56)^2\ \mathrm{GeV}^2. \tag{22}$$

4 Cross sections for mirror fermion production

Heavy mirror fermion production in high energy ep collisions is made possible by the mixing of ordinary and mirror fermions. The corresponding vertex and the lowest order Feynman-diagrams for mirror fermion production in electron-proton scattering is shown by Fig. 1. Figure 1b refers to mirror lepton production and Fig. 1c to mirror quark production. In this section we present the cross-sections of mirror fermion production.

Using the notations of Sect. 2, the production cross-section of the mirror electron-neutrino on a u-quark in the proton is

$$\frac{d\sigma_{e^-u\to N_e d}}{dQ^2}=\frac{g^4}{512\pi(M_W^2+Q^2)^2}\cdot\Big\{[\sin^2(\alpha_{1l}-\alpha_{2l})+\sin^2(\alpha_{1l}+\alpha_{2l})]\cdot[\cos^2(\alpha_{2q}-\alpha_{1q})+\cos^2(\alpha_{2q}+\alpha_{1q})]\cdot\left[1+(1-y)^2-\frac{M^2}{xs}(2-y)\right]+4\sin(\alpha_{1l}-\alpha_{2l})\sin(\alpha_{1l}+\alpha_{2l})\cdot\cos(\alpha_{2q}-\alpha_{1q})\cos(\alpha_{2q}+\alpha_{1q})\left[1-(1-y)^2-\frac{M^2y}{xs}\right]\Big\}. \tag{23}$$

Similarly, the cross-section of heavy mirror electron production on u- and d-quarks is ($A=1$ stands for u-quark, $A=2$ for d-quark)

$$\frac{d\sigma_{e^-q_A\to E^-q_A}}{dQ^2}=\frac{(g^2+g'^2)^2}{2048\pi(M_Z^2+Q^2)^2}\cdot\sin^2(2\alpha_{2l})\cdot[1+\cos^2(2\alpha_{Aq})]\left[1+(1-y)^2-\frac{M^2}{xs}(2-y)\right]. \tag{24}$$

All the masses, except for those of the vector mesons (M_W, M_Z) and the heavy mirror fermion (M) have been

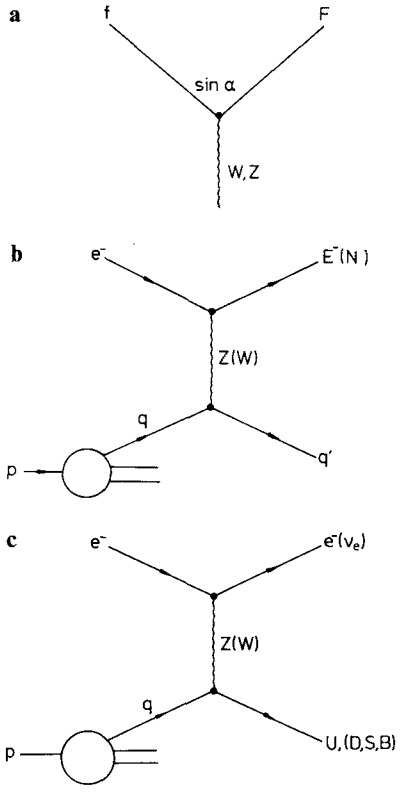

Fig. 1. **A** The mixing vertex between the light fermion (f) and its mirror partner (F). f and F have the same quantum numbers, apart from the exchange of left- and right-handed chiral components. **B** The lowest order Feynman-graph in ep scattering for the production of the mirror electron E (electron-neutrino: N_e) through the mixing vertex in **A**. **C** The lowest order Feynman-graph in ep scattering for the production of the mirror quarks (U, D, S, B) through the mixing vertex in **A**

taken to be zero. x is the Bjorken-variable of the initial parton. Denoting the 4-momentum of the electron, mirror-lepton and initial parton, respectively, by p_e, P and xp, the usual kinematical variables are defined as

$$s=(p+p_e)^2; \quad q=p_e-P; \quad Q^2=-q^2; \quad y=\frac{p\cdot q}{p\cdot q_e}. \tag{25}$$

The kinematical limits are given by

$$1\geqq x\geqq x_{\min}\equiv\frac{M^2}{s}; \quad 0\leqq y\leqq y_{\max}\equiv 1-\frac{x_{\min}}{x} \tag{26}$$

and Q^2 is expressed as $Q^2=xys$.

In the production cross-sections of mirror electron and mirror electron-neutrino in (23–24) three different functions of the mirror mixing angles occur. Since, however, all the angles are small, one can approximate $\sin\alpha$ by α and $\cos\alpha$ by 1. In this case (23) can be written as

$$\frac{d\sigma_{e^-u\to N_e d}}{dQ^2}\simeq\frac{g^4}{64\pi(M_W^2+Q^2)^2}\cdot\left[\alpha_{1l}^2\left(1-\frac{M^2}{xs}\right)+\alpha_{2l}^2(1-y)\left(1-y-\frac{M^2}{xs}\right)\right]. \tag{27}$$

In the same approximation (24) is

$$\frac{d\sigma_{e^-q_A\to E^-q_A}}{dQ^2}\simeq\frac{(g^2+g'^2)^2}{256\pi(M_Z^2+Q^2)^2}\alpha_{2l}^2\left[1+(1-y)^2-\frac{M^2}{xs}(2-y)\right]. \tag{28}$$

The laboratory frame kinematics of the produced mirror lepton is given as follows. Transverse momentum conservation implies that the transverse momentum of the final parton is opposite to the transverse momentum of the produced mirror lepton. The magnitude of both of them is

$$p_T=\sqrt{xys\left(1-y-\frac{M^2}{xs}\right)}. \tag{29}$$

If in the laboratory frame the electron energy is $E_{\rm el}$ and the proton energy is $E_{\rm pr}$, moreover the proton goes forward, then the longitudinal (i.e. parallel to the proton) momentum of the mirror lepton is given by

$$P_L=E_{\rm pr}x\left(y+\frac{M^2}{xs}\right)-E_{\rm el}(1-y) \tag{30}$$

and the struck parton in the final state has a longitudinal momentum

$$p'_L=E_{\rm pr}x\left(1-y-\frac{M^2}{xs}\right)-E_{\rm el}y. \tag{31}$$

This shows that in most mirror lepton production events there is also a high transverse momentum jet originating from the struck parton.

Quite similar formulae are obtained for the production cross-sections of mirror quarks. The production cross-section of the mirror d-quark (D) on a u-quark in the proton is

$$\frac{d\sigma_{e^-u\to\nu_e D}}{dQ^2}=\frac{g^4}{512\pi(M_W^2+Q^2)^2}|M_{11}|^2\cdot\Big\{[\sin^2(\alpha_{1q}-\alpha_{2q})+\sin^2(\alpha_{1q}+\alpha_{2q})]\cdot[\cos^2(\alpha_{2l}-\alpha_{1l})+\cos^2(\alpha_{2l}+\alpha_{1l})]\left[1+(1-y)^2-\frac{M^2}{xs}y\right]+4\sin(\alpha_{1q}-\alpha_{2q})\sin(\alpha_{1q}+\alpha_{2q})\cos(\alpha_{2l}-\alpha_{1l})\cdot\cos(\alpha_{2l}+\alpha_{1l})\left[1-(1-y)^2-\frac{M^2}{xs}(2-y)\right]\Big\}. \tag{32}$$

Assuming family independent mirror mixing angles, the mirror s-quark (S) and mirror b-quark (B) production cross-sections are given by the same expressions (except that M denotes the mass of the appropriate mirror quark) multiplied by the ratio of the squares of the relevant Kobayashi-Maskawa matrix elements. For S production e.g. we have:

$$\frac{d\sigma_{e^-u\to\nu_e S}}{dQ^2}=\frac{d\sigma_{e^-u\to\nu_e D}}{dQ^2}\frac{|M_{12}|^2}{|M_{11}|^2}. \tag{33}$$

Assuming family dependent mirror mixing angles the above equation should be modified taking into account the changes in the mirror mixing angle factors. The changes should be obvious from (7).

The cross-section of heavy mirror u-quark (U) production on u-quarks is:

$$\frac{d\sigma_{e^-u\to e^-U}}{dQ^2}=\frac{(g^2+g'^2)^2}{2048\pi(M_Z^2+Q^2)^2}$$
$$\cdot\sin^2(2\alpha_{1q})[1+\cos^2(2\alpha_{2l})]\left[1+(1-y)^2-\frac{M^2}{xs}\right]. \quad (34)$$

The mirror d-quark (D) production cross-section on d-quarks is given by the same expression (except that M denotes the mass of D) multiplied by a factor containing the mirror mixing angles. We have:

$$\frac{d\sigma_{e^-d\to e^-D}}{dQ^2}=\frac{d\sigma_{e^-u\to e^-U}}{dQ^2}\frac{\sin^2(2\alpha_{2q})}{\sin^2(2\alpha_{1q})}. \quad (35)$$

All the masses, except for those of the vector mesons (M_W, M_Z) and the heavy mirror fermion (M) have been again taken to be zero. The kinematics for mirror quark production is not the same as in case of mirror lepton production. Denoting the 4-momentum of the electron, struck-lepton, initial parton and the mirror quark by p_e, p_l', xp and P respectively, the usual kinematical variables are defined as

$$s=(p+p_e)^2;\quad q=p_e-p_l';\quad Q^2=-q^2;\quad y=\frac{p\cdot q}{p\cdot p_e}. \quad (36)$$

The kinematical limits are given by

$$1\geqq x\geqq x_{\min}\equiv\frac{M^2}{s};\quad 1\geqq y\geqq y_{\min}\equiv\frac{x_{\min}}{x}, \quad (37)$$

and Q^2 is expressed as $Q^2=xys-M^2$.

In the small mixing angle approximation the mirror quark production cross-sections of (32), 34) are given by

$$\frac{d\sigma_{e^-u\to\nu_eD}}{dQ^2}\simeq\frac{g^4}{64\pi(M_W^2+Q^2)^2}|M_{11}|^2$$
$$\cdot\left[\alpha_{1q}^2\left(1-\frac{M^2}{xs}\right)+\alpha_{2q}^2(1-y)\left(1-y+\frac{M^2}{xs}\right)\right] \quad (38)$$

and

$$\frac{d\sigma_{e^-u\to e^-U}}{dQ^2}\simeq\frac{(g^2+g'^2)^2}{256\pi(M_Z^2+Q^2)^2}\alpha_{2q}^2\left[1+(1-y)^2-\frac{M^2}{xs}\right]. \quad (39)$$

Equations (33), (35) remain unchanged in the small angle approximation.

The laboratory frame kinematics of the produced mirror quarks is also different from that of the mirror lepton case. Transverse momentum conservation implies that the transverse momentum of the final lepton is opposite to the transverse momentum of the produced mirror quark. The magnitude of both of them is

$$p_T=\sqrt{(1-y)(xys-M^2)}. \quad (40)$$

In the laboratory frame the longitudinal (i.e. parallel to the proton) momentum of the mirror quark is given by

$$P_L=-yE_{\rm el}+xE_{\rm pr}(1-y)+\frac{M^2}{4E_{\rm el}}, \quad (41)$$

and the struck lepton in the final state has a longitudinal momentum

$$(p_l')_L=-E_{\rm el}(1-y)+yxE_{\rm pr}-\frac{M^2}{4E_{\rm el}}. \quad (42)$$

This shows that in most mirror quark production events both the mirror quark and the struck lepton have high transverse momentum.

Due to the vector boson propagators squared both the mirror lepton and mirror quark production cross-sections are dominated by small x- and y-values, but a strong peak at small Q^2 characteristic for photon exchange reactions is absent. (Note that the mixing vertex in Fig. 1a does not exist for photons.) As a consequence, the total cross-section is not sensitive to a cut at small Q^2, which is needed for the applicability of the parton model. In the following the low Q^2 cut will be always taken to be 5 GeV^2 and the structure functions of Eichten et al. will be used [21]. (The cross-sections are also not sensitive to the angular cuts around the beam directions.) The total production cross-section and the average transverse momentum for N_e, E^-, ν_eD, eU, eD production at $\sqrt{s}=314$, 566, 1400 GeV is given in Tables 1–5 respectively. The first energy is typical for HERA with 30 GeV electrons on 820 GeV protons. The second one is a possible HERA upgrade with 40 GeV electrons on 2 GeV protons and the third is in the range of LEP/

Table 1. Total production cross-section (σ) and average transverse momentum ($\langle p_T\rangle$) of the mirror electron-neutrino in ep collisions at energies $\sqrt{s}=314$, 566, 1400 GeV as a function of the mirror electron-neutrino mass M (in GeV). For simplicity, both mixing angle squared appearing in (27) are assumed here to be 0.02. The cross-sections are in 10^{-2} pb, the transverse momenta in GeV

M	$\sqrt{s}=314$ σ	$\sqrt{s}=314$ $\langle p_T\rangle$	$\sqrt{s}=566$ σ	$\sqrt{s}=566$ $\langle p_T\rangle$	$\sqrt{s}=1400$ σ	$\sqrt{s}=1400$ $\langle p_T\rangle$
100	31.40	34.92	109.7	51.60	288.28	72.01
120	19.22	32.96	88.45	50.97	261.89	72.55
140	10.99	30.59	70.45	50.03	238.21	72.85
160	5.77	27.98	55.4	48.84	216.81	72.95
180	2.72	25.10	42.94	47.47	197.42	72.89
200	1.11	22.06	32.76	45.94	179.80	72.69
250	–	–	15.31	41.58	142.10	71.76
300	–	–	6.13	36.65	111.79	70.35
350	–	–	1.98	31.23	87.29	68.61
400	–	–	0.444	25.87	67.52	66.61
450	–	–	0.056	19.66	51.59	64.42
500	–	–	0.002	12.94	38.86	62.07

Table 2. The same as Table 1, for the mirror electron production

M	$\sqrt{s}=314$ σ	$\sqrt{s}=314$ $\langle p_T\rangle$	$\sqrt{s}=566$ σ	$\sqrt{s}=566$ $\langle p_T\rangle$	$\sqrt{s}=1400$ σ	$\sqrt{s}=1400$ $\langle p_T\rangle$
100	12.25	35.94	47.33	53.81	139.3	76.25
120	7.35	33.95	37.64	53.30	125.4	77.03
140	4.11	31.56	29.59	52.45	113.05	77.52
160	2.11	28.88	22.98	51.31	102.0	77.80
180	0.97	25.97	17.59	49.94	92.1	77.88
200	0.39	22.83	13.26	48.40	83.3	77.79
250	–	–	6.00	43.90	64.6	77.06
300	–	–	2.32	38.82	49.94	75.76
350	–	–	0.72	33.17	38.38	74.05
400	–	–	0.16	27.33	29.24	72.03
450	–	–	0.02	20.98	22.01	69.81
500	–	–	–	–	16.35	67.37

Table 3. The same as Table 1, for the ν_e+mirror d-quark production

M	$\sqrt{s}=314$ σ	$\sqrt{s}=314$ $\langle p_T\rangle$	$\sqrt{s}=566$ σ	$\sqrt{s}=566$ $\langle p_T\rangle$	$\sqrt{s}=1400$ σ	$\sqrt{s}=1400$ $\langle p_T\rangle$
100	31.63	35.11	106.5	53.37	317.81	72.05
120	18.43	34.34	83.38	54.18	243.86	72.57
140	11.43	29.40	72.60	52.21	234.59	72.88
160	5.79	27.88	54.51	50.77	228.67	73.04
180	2.72	24.07	43.56	46.82	177.81	72.96
200	0.91	22.80	31.94	46.15	158.89	72.79
250	–	–	15.10	43.0	135.07	71.76
300	–	–	6.58	32.27	97.158	70.38
350	–	–	1.38	30.16	77.37	68.66
400	–	–	0.41	29.45	63.51	66.69
450	–	–	0.06	18.80	54.28	64.63
500	–	–	0.002	12.72	42.39	61.89

Table 4. The same as Table 1, for e+mirror u-quark production

M	$\sqrt{s}=314$ σ	$\sqrt{s}=314$ $\langle p_T\rangle$	$\sqrt{s}=566$ σ	$\sqrt{s}=566$ $\langle p_T\rangle$	$\sqrt{s}=1400$ σ	$\sqrt{s}=1400$ $\langle p_T\rangle$
100	7.68	37.88	30.23	55.11	85.19	79.01
120	4.31	37.74	22.63	57.47	76.35	81.74
140	2.49	32.42	18.66	52.38	72.72	80.85
160	1.26	29.33	14.10	52.38	64.23	80.07
180	0.56	27.62	10.90	51.50	55.20	83.40
200	0.21	25.98	7.82	51.40	53.31	79.66
250	–	–	3.59	44.47	42.96	80.43
300	–	–	1.25	42.35	29.45	78.29
350	–	–	0.52	31.17	24.03	77.20
400	–	–	0.08	29.28	17.58	75.83
450	–	–	0.01	19.86	11.78	72.08
500	–	–	0.003	14.28	8.88	71.39

LHC [22]. As a typical example all the squared mixing angles have been assumed to be 0.02 in the tables.

Given the cross-sections in Tables 1–5 and assuming an integrated luminosity of 100 pb^{-1} the discovery of mirror leptons and mirror quarks seems to be possible. At HERA the mass discovery limit is very roughly 200 GeV, at the upgraded HERA it is 300–350 GeV,

Table 5. The same as Table 1, for the e^-+mirror d-quark production

M	$\sqrt{s}=314$ σ	$\sqrt{s}=314$ $\langle p_T\rangle$	$\sqrt{s}=566$ σ	$\sqrt{s}=566$ $\langle p_T\rangle$	$\sqrt{s}=1400$ σ	$\sqrt{s}=1400$ $\langle p_T\rangle$
100	2.69	34.18	12.55	53.29	48.89	69.95
120	1.30	35.33	9.29	53.57	40.068	75.72
140	0.71	30.03	7.14	50.59	32.44	75.38
160	0.32	28.05	5.11	50.56	30.36	76.93
180	0.13	24.71	3.577	50.53	31.49	73.95
200	–	–	2.43	50.88	27.51	72.57
250	–	–	0.985	45.46	17.29	71.42
300	–	–	0.42	38.69	12.74	70.71
350	–	–	0.08	35.27	10.07	67.38
400	–	–	0.014	27.87	6.34	67.61
450	–	–	0.002	16.66	4.69	67.53
500	–	–	–	–	3.27	67.40

while for the LEP/LHC e-p option we estimate 500 GeV. In view of the unitarity bounds derived in Sect. III the physically plausible region is then covered. The average transverse momentum of the mirror fermions is large, the p_T balance is given by the struck quark or the struck lepton in the mirror lepton and mirror quark cases respectively. Thus in both cases one has two large transverse momentum particles (jets) in the final state acompanied by the remnant of the initial proton, (which of course has low p_T).

5 Mirror decay and the final states

Depending on the relations between the masses the decay patterns of mirror fermions may be different. The heavier member of a mirror doublet can always decay into the lighter one + a pair of ordinary fermions or a vector boson. Such type of decays are not suppressed by factors containing the mixing angles, moreover the (essentially) $V+A$ structure of the mirror fermion-vector boson coupling directs these decays. However, if the mass differences within the mirror doublets are small the rates will also be small [1]. As a simple scheme we shall assume in the following (almost) degenerate mirror doublets. In this case the decay is made possible by the mixing with ordinary fermions. (The lighter particle within a mirror doublet will decay anyhow in this way.) For heavy mirror fermions the dominant decay modes are the two body decays into a vector boson and an ordinary fermion [1]. Thus we have:

$$N_e \to e^- + W^+, \nu_e + Z \qquad E^- \to e^- + Z, \nu_e + W^-$$
$$U \to d + W^+, s + W^+, b + W^+, u + Z^0$$
$$D \to u + W^-, d + Z^0 \tag{43}$$

and similarly for the other mirror families. The corresponding widths are:

$$\Gamma_{E^- \to \nu_e W^-} = M_E \frac{g^2}{128\pi}\left(1 - \frac{M_W^2}{M_E^2}\right)\left(1 - 2\frac{M_W^2}{M_E^2} + \frac{M_E^2}{M_W^2}\right)$$
$$\cdot(\sin^2(\alpha_{2l} + \alpha_{1l}) + \sin^2(\alpha_{2l} - \alpha_{1l})),$$

$$\Gamma_{E^-\to e^- Z^0} = M_E \frac{g^2}{256\pi\cos^2\Theta_W}\left(1-\frac{M_Z^2}{M_E^2}\right)$$
$$\cdot\left(1-2\frac{M_Z^2}{M_E^2}+\frac{M_E^2}{M_Z^2}\right)\sin^2(2\alpha_{2l})$$

$$\Gamma_{N_e\to e^- W^+} = M_N \frac{g^2}{128\pi}\left(1-\frac{M_W^2}{M_N^2}\right)\left(1-2\frac{M_W^2}{M_N^2}+\frac{M_N^2}{M_W^2}\right)$$
$$\cdot(\sin^2(\alpha_{2l}+\alpha_{1l})+\sin^2(\alpha_{2l}-\alpha_{1l})),$$

$$\Gamma_{N_e\to\nu_e Z^0} = M_N \frac{g^2}{256\pi\cos^2\Theta_W}\left(1-\frac{M_Z^2}{M_N^2}\right)$$
$$\cdot\left(1-2\frac{M_Z^2}{M_N^2}+\frac{M_N^2}{M_Z^2}\right)\sin^2(2\alpha_{1l})$$

$$\Gamma_{U\to dW^+} = M_U \frac{g^2}{128\pi}\left(1-\frac{M_W^2}{M_U^2}\right)\left(1-2\frac{M_W^2}{M_U^2}+\frac{M_U^2}{M_W^2}\right)$$
$$\cdot(\sin^2(\alpha_{2q}+\alpha_{1q})+\sin^2(\alpha_{2q}-\alpha_{1q}))\,|M_{11}|^2$$

$$\Gamma_{U\to uZ^0} = M_U \frac{g^2}{256\pi\cos^2\Theta_W}\left(1-\frac{M_Z^2}{M_U^2}\right)$$
$$\cdot\left(1-2\frac{M_Z^2}{M_U^2}+\frac{M_U^2}{M_Z^2}\right)\sin^2(2\alpha_{1q})$$

$$\Gamma_{D\to uW^-} = M_D \frac{g^2}{128\pi}\left(1-\frac{M_W^2}{M_D^2}\right)\left(1-2\frac{M_W^2}{M_D^2}+\frac{M_D^2}{M_W^2}\right)$$
$$\cdot(\sin^2(\alpha_{2q}+\alpha_{1q})+\sin^2(\alpha_{2q}-\alpha_{1q}))\,|M_{11}|^2$$

$$\Gamma_{D\to dZ^0} = M_U \frac{g^2}{256\pi\cos^2\Theta_W}\left(1-\frac{M_Z^2}{M_D^2}\right)$$
$$\cdot\left(1-2\frac{M_Z^2}{M_D^2}+\frac{M_D^2}{M_Z^2}\right)\sin^2(2\alpha_{2q}). \tag{44}$$

The formulae involving s or b should be evident. Similar formulae hold for the decay widths of mirror fermions of other families.

When $M_E = M_N$

$$\Gamma_{N_e\to\nu_e Z^0} = \Gamma_{E^-\to e^- Z^0}\frac{\sin^2 2\alpha_{1l}}{\sin^2 2\alpha_{2l}} \qquad \Gamma_{N_e\to e^- W^+} = \Gamma_{E^-\to\nu_e W^-}. \tag{45}$$

When $M_U = M_D$

$$\Gamma_{U\to uZ^0} = \Gamma_{D\to dZ^0}\frac{\sin^2 2\alpha_{1q}}{\sin^2 2\alpha_{2q}} \qquad \Gamma_{U\to dW^+} = \Gamma_{D\to uW^-}. \tag{46}$$

E.g. for $M_N = M_E = M_U = M_D = 150$ GeV and all squared mirror mixing angles equal to 0.02 we obtain:

$$\Gamma_{N_e\,\mathrm{tot}} = \Gamma_{E^-\,\mathrm{tot}} = \Gamma_{U\,\mathrm{tot}} = \Gamma_{D\,\mathrm{tot}} \approx 50\ \mathrm{MeV}. \tag{47}$$

The decay channels in (46) have a general mixture of vector and axial-vector couplings depending on the relative magnitude of the mixing angles. Thus establishing the mirror fermion character of the decaying particles is not easy.

Combining the above decay modes with the mirror fermion production possibilities at ep collisions we obtain the processes:

$$e^-, p\to E^-,$$
$$\text{jet}\begin{matrix}\nearrow e^-, Z^0,\ \text{jet}\to e^-, l^+, l^-, \text{jet}; e^-, \bar\nu, \nu, \text{jet}; e^-, 3\,\text{jet}\\ \searrow \nu_e, W^-, \text{jet}\to \nu_e, l^-, \bar\nu_l, \text{jet}; \nu_e, 3\,\text{jet}\end{matrix}$$

$$e^-, p\to N_e,$$
$$\text{jet}\begin{matrix}\nearrow \nu_e, Z^0,\ \text{jet}\to \nu_e, l^+, l^-, \text{jet}; \nu_e, \bar\nu, \nu, \text{jet}; \nu_e, 3\,\text{jet}\\ \searrow e^-, W^+, \text{jet}\to e^-, l^+, \nu_l, \text{jet}; e^-, 3\,\text{jet}\end{matrix}$$

$$e^-, p\to \nu_e,$$
$$D\begin{matrix}\nearrow \nu_e, Z^0,\ \text{jet}\to \nu_e, l^+, l^-, \text{jet}; \nu_e, \bar\nu, \nu, \text{jet}; \nu_e, 3\,\text{jet}\\ \searrow \nu_e, W^-, \text{jet}\to \nu_e, l^-, \nu_l, \text{jet}; \nu_e, 3\,\text{jet}\end{matrix}$$

$$e^-, p\to e^-,$$
$$U\begin{matrix}\nearrow e^-, Z^0,\ \text{jet}\to e^-, l^+, l^-, \text{jet}; e^-, \bar\nu, \nu, \text{jet}; e^-, 3\,\text{jet}\\ \searrow e^-, W^+, \text{jet}\to e^-, l^+, \nu_l, \text{jet}; e^-, 3\,\text{jet}\end{matrix}$$

$$e^-, p\to e^-,$$
$$D\begin{matrix}\nearrow e^-, Z^0,\ \text{jet}\to e^-, l^+, l^-, \text{jet}; e^-, \bar\nu, \nu, \text{jet}; e^-, 3\,\text{jet}\\ \searrow e^-, W^-, \text{jet}\to e^-, l^-, \bar\nu_l, \text{jet}; e^-, 3\,\text{jet}.\end{matrix} \tag{48}$$

In the above processes the proton fragment jet (which goes in the beam direction anyway) has been omitted everywhere on the right hand sides, i.e. only the four high transverse momentum particles (jets) were written out. From the point of view of experimental observation the channels with three charged leptons + jet (all high p_T), or two charged leptons + one neutrino + one jet (all high p_T) are the best. In the case of three high p_T charged leptons the reconstruction of the mirror fermion mass from the final state momenta should be possible. This opportunity is open for the E^- and U, D production.

Possible background processes for mirror fermions in ep collisions are the second order weak vector boson production (see [23, 24] and references therein) and, in case of final states with three jets, QCD multijet production. Both these processes are, however, dominated by photon exchange and hence by low Q^2. The second order weak vector boson production has altogether small cross-sections in the order of a few times 10^{-2} pb, even for a low Q^2 cut at 4 GeV^2 [23, 25]. The discriminating feature of mirror fermion production is the presence of four large transverse momenta in the final state. In this kinematical range the QCD process is expected to be negligible. (In the leptonic channels the QCD background is, of course, absent.)

Assuming the heavy top quark's mass to be close to the mirror masses, top production via gluon – vector boson fusion is also a possible background. At HERA energies the cross-section is negligible [26], but at LEP/LHC it is comparable to the mirror fermion production cross-section [27]. Strictly speaking the final state is different (namely $\nu_e \bar b W^- b$(+the target jet)). However, the final state b jet has very often small transverse momentum, so it can not be distinguished from the target jet [27]. It is important to realize that in case of mirror

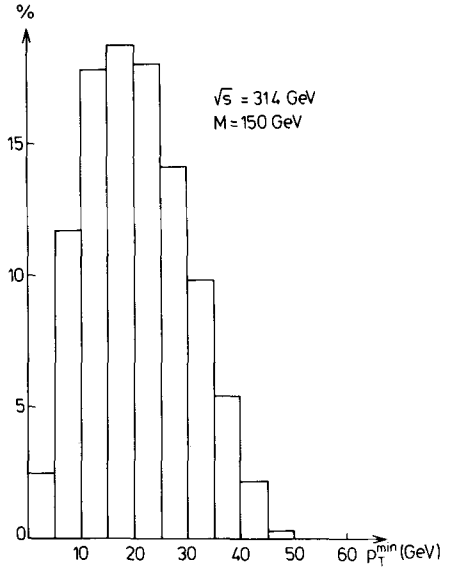

Fig. 2. The distribution of the smallest out of the four transverse momenta of the leptons and/or jets in the final state of the process $ep \to E^-$ jet and mirror decay through the Z for a mirror electron mass $M = 150$ GeV at $\sqrt{s} = 314$ GeV

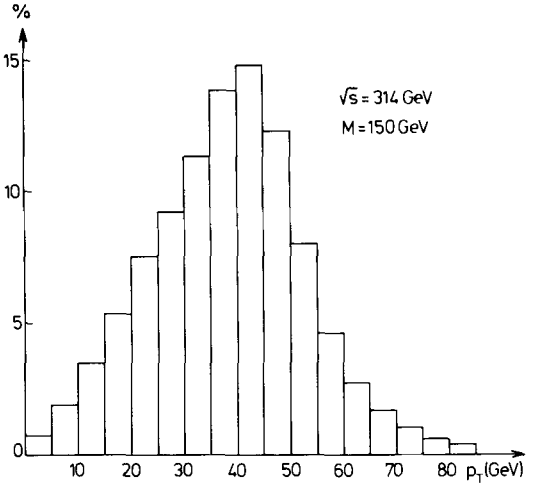

Fig. 3. The inclusive distribution of the neutrino transverse momentum in the process $ep \to eN_e$; $N_e \to \nu_e Z$ or $N_e \to e^- W^+ \to e^- e^+ \nu_e$ for a mirror electron-neutrino mass $M = 150$ GeV at $\sqrt{s} = 314$ GeV

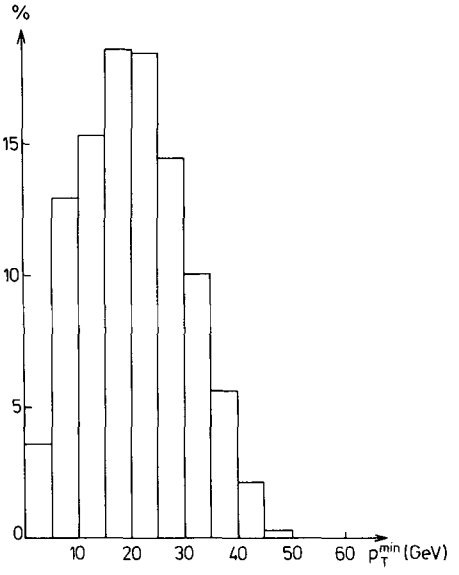

Fig. 4. The distribution of the smallest out of the four transverse momenta of the leptons and/or jets in the final state of the process $ep \to e^- U$ and mirror decay for a mirror u-quark mass $M = 150$ GeV at $\sqrt{s} = 314$ GeV

production the $\nu_e W^-$ *jet final state is always accompanied by other final states* ($e^- Z^0$ jet, or $\nu_e Z^0$ jet) which after vector boson decay have "better" final states than the one of top production, (which either contains two neutrinos or three high p_T jets).

We have studied the final state distributions by a Monte Carlo program generating the mirror fermions according to (23), (24), (32), (34), (35). The decays of the mirror fermion into a light fermion and a vector boson were averaged equally over the mirror fermion helicities (small polarization effects were neglected here). A few of the distributions calculated are shown in Figs. 2–7.

Figure 2 shows the distribution of the smallest of the four transverse momenta in the representative case of the $e^- Z^0$ final state of E^- production, with a mirror electron mass $M = 150$ GeV and $\sqrt{s} = 314$ GeV. The distribution peaks around 20 GeV showing that all the four transverse momenta of the final state are high. The average of the minimal p_T is 20.58 GeV. As one can see on the figure, in about 85% of the cases all four transverse momenta are larger than 10 GeV, and roughly 50% of the events is above a minimal transverse momentum of 20 GeV.

Since neutrinos can be indirectly detected by the transverse momentum inbalance in the final state, an interesting question is the distribution of the neutrino transverse momentum in the heavy mirror lepton production events. Such a distribution is shown on the example of the $N_e \to e^- + W^+$ final state for a mirror neutrino mass $M = 150$ GeV in Fig. 3. The distribution is peaked around 45 GeV, the average is 38.46 GeV. A typical cut at 20 GeV leaves still more than 88% of the events.

To plot characteristics of final states of mirror quark production we choose the same mass and energy as for mirror lepton production. Figure 4 shows the $p_{T_{min}}$ in Ue^- production. The peak is around 20 GeV, while the average is 20.6 GeV. A 10 GeV cut leaves 84% of the events. Figure 5 shows the distribution of minimal transverse momentum in $D\nu_e$, De^- production. The peak is around 20 GeV, the average is 19.7 GeV, 82% lies above 10 GeV. Figure 6 presents the p_T distribution of $D(\nu_e)$ in $D\nu_e$ production. The peak is around 25 GeV, the average is 28.63 GeV. 88% of the events has higher transverse momentum than 10 GeV. The p_T distribution of ν_e in Ue^- production and subsequent U decay into $de^+\nu_e$ is shown in Fig. 7. The distribution peaks around 30 GeV, the average is 39.3 GeV, while 97% has more than 10 GeV. In general the p_T distributions in the mir-

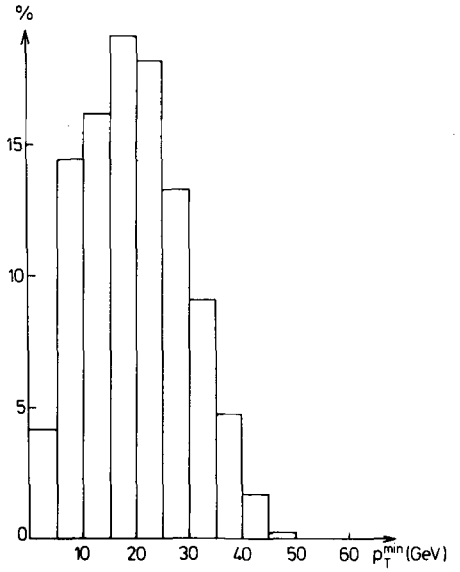

Fig. 5. The distribution of the smallest out of the four transverse momenta of the leptons and/or jets in the final state of the process $ep \to e^- D$ or $\nu_e D$ and mirror decay for a mirror d-quark mass $M = 150$ GeV at $\sqrt{s} = 314$ GeV

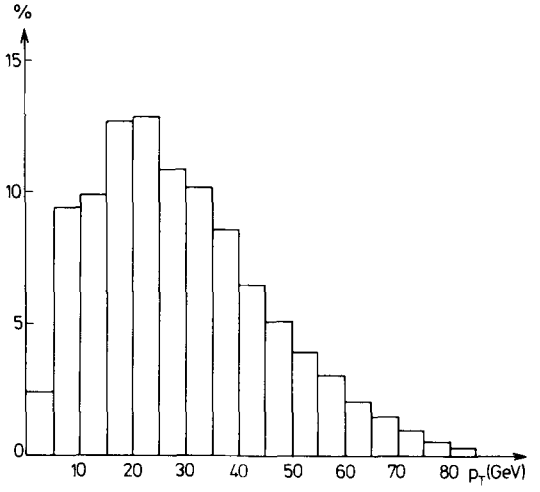

Fig. 6. The inclusive distribution of the mirror d-quark (ν_e) transverse momentum in the process $ep \to \nu_e D$ for a mirror d-quark mass $M = 150$ GeV at $\sqrt{s} = 314$ GeV

ror quark case are quite similar to those of the mirror lepton case if the mirror masses are taken to be the same.

We have studied several other final state distributions, too. (The Monte Carlo program generating the final states with mirror fermions can be obtained from the author upon request.) The conclusion of this Monte Carlo study was that the transverse momenta alone give very distinctive signatures. These informations together with the peaks in the invariant masses are certainly enough to recognize a large fraction of such events above any conventional background. As the tables show, for mixing angles of the order of the present upper limits (9) an integrated luminosity of 100 pb^{-1} at HERA suf-

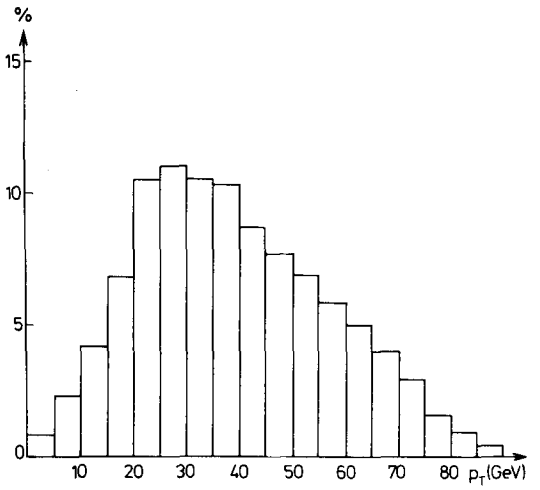

Fig. 7. The inclusive distribution of the neutrino transverse momentum in the process $ep \to e^- U \to e^- W^+$ jet $\to e^- l^+ \nu_l$ jet for a mirror u-quark mass $M = 150$ GeV at $\sqrt{s} = 314$ GeV

fices for the discovery of mirror leptons roughly up to a mass of 200 GeV. The HERA-upgrade could go up to 300–350 GeV, and LEP/LHC up to the unitarity limit for the heavy fermion Yukawa-coupling at a mass of about 500 GeV.

6 Summary

In this paper we have studied the production and decay properties of mirror fermions in ep collisions at high energies. As a prototype model we have choosen the hermitian mirror fermion model of [1]. To obtain a rough idea on the possible masses of mirror fermions we have derived mass bounds imposing the partial wave unitarity condition to mirror fermion scattering amplitudes calculated in the tree graph approximation. The bounds are very similar to the bounds on ordinary heavy fermions obtained in [19]. The results for the various cases are collected in (14)–(22). If tree unitarity is a good approximation one does not expect mirror fermion masses to be larger than 500 GeV. Moreover, to get a lower bound we have assumed that mirror fermions will not be found at LEP.

The cross-sections for mirror fermion production in ep collisions are given in (23), (24), (32), (34), (35). Assuming equal squared mirror mixing angles of the magnitude 0.02 the total production cross-sections are given in Tables 1–5 for HERA ($\sqrt{s} = 314$ GeV) a possible HERA upgrade ($\sqrt{s} = 566$ GeV) and the LEP/LHC ep option ($\sqrt{s} = 1400$ GeV), for a range of mirror fermion masses. Based on these cross-sections the discovery limits for the three different energies are 200 GeV, 300–350 GeV and 500 GeV respectively, assuming 100 pb^{-1} integrated luminosity. Strictly speaking, if mirror fermions will not be found at the ep colliders, combined limits on the mixing angles and masses may be established. In this case mirror fermions may be discovered at hadronic colliders

(SSC, LHC), where they may be pair produced at higher energies than at the e^+e^- colliders. For the TEVATRON the pair production cross-section for mirror leptons is small. E.g. for a 4.4 pb^{-1} integrated luminosity (the 1988–89 one year run) the prediction (ignoring cuts) is 0.9 (0.4) mirror electron pairs assuming 100 GeV (120 GeV) for the mirror mass. Though mirror quark production has larger cross-section, the large backgrounds make mirror quark detection even more difficult.

The properties of the final state after mirror and vector boson decay have been studied for the case of (almost) degenerate heavy mirror doublets, decaying dominantly to a vector boson and a light fermion. The possible final states are collected in (48). The final states consist of four high p_T leptons or jets and the target jet. The final state distributions have been studied by a Monte Carlo event generator. Various distributions are plotted in Figs. 2–7. Obviously the best channels for the discovery of mirror particles are those containing leptons. For E^- production the best channel is $(e^- l^+ l^-)$ jet + target jet, where the particles in parenthesis are the decay products of E^-. For N_e production the best channel is $(\nu_e l^+ l^-)$ jet + target jet. For U and D production the best channels are $\nu_e(l^+ l^-$ jet) + target jet and $e^-(l^+ l^-$ jet) + target jet. In these cases the invariant mass of the decaying mirror fermion can be reproduced from the final state momenta.

In summary, the high energy ep colliders have a good capability to discover the heavy mirror fermions, or at least give important lower limits for their masses and upper limits for their mixing with ordinary fermions.

Acknowledgements. I thank Dr. I. Montvay for initiating my interest in the subject, continuous encouragement and a careful reading of the manuscript. The hospitality of the DESY Theory group during the preparation of the paper is gratefully acknowledged.

References

1. I. Montvay: Phys. Lett. 205 B (1988) 315
2. D.J. Gross, R. Jackiw: Phys. Rev. D6 (1972) 477; P. Fayet: In: Proceedings of the 17th Rencontre de Moriond on elementary particles. J. Tran Thanh Van (ed.) p. 483. Gif-sur-Yvette: Editions Frontiers 1982
3. G. Senjanovic, F. Wilczek, A. Zee: Phys. Lett. 141 B (1984) 389
4. E. Witten: Nucl. Phys. B186 (1981) 412
5. F. de Aguila et al.: Nucl. Phys. B250 (1985) 225
6. A.L. Kagan: Maryland preprint, UMDEPP 89-109
7. J. Maalampi, M. Roos: Phys. Rep. 186 (1990) 53
8. H.B. Nielsen, M. Ninomiya: Nucl. Phys. B185 (1981) 20; errata: Nucl. Phys. B195 (1982) 541
9. I. Montvay: Nucl. Phys. B307 (1988) 389
10. I. Montvay: Heavy Flavours and High Energy Collisions in the 1–100 Tev Range, Proceedings of the 7th Eloisatron Project Workshop, Erice, June 1988. A. Ali, L. Cifarelli (eds.) p. 469. New York: Plenum Press 1989
11. K. Farakos et al.: preprint DESY 90-035 (1990)
12. C. Wagner: PhD Thesis, University of Hamburg, 1989, preprint DESY 89-083
13. K. Farakos, G. Koutsoumbas, I. Montvay: Z. Phys. C – Particles and Fields 47 (1990) (641)
14. A. Borrelli et al.: Phys. Lett. 221 B (1989) 360; Università di Roma preprint, n. 655, 1989
15. P. Langacker, D. London: Phys. Rev. D38 (1988) 886
16. J. Maalampi, M. Roos: Z. Phys. C – Particles and Fields 14 (1989) 319
17. F. Csikor, I. Montvay: Phys. Lett. 231 B (1989) 503
18. I. Montvay: Proc. of the Int. Europhys. Conf. on High Energy Physics, Madrid, 1989
19. M.S. Chanowitz, M.A. Furman, I. Hinchliffe: Phys. Lett. 78 B (1978) 285; Nucl. Phys. B153 (1979) 402
20. M. Lüscher, P. Weisz: Phys. Lett. 212 B (1988) 472
21. E. Eichten, I. Hinchliffe, K. Lane, C. Quigg: Rev. Mod. Phys. 56 (1984) 579; ibid. 58 (1986) 1047
22. Proceedings of the Workshop on Physics at Future Accelerators. La Thuile (1987), CERN 87-07
23. K.J.F. Gaemers, R.M. Godbole, M. van der Horst: In: Proceedings of the HERA Workshop. R.D. Peccei (ed.) Vol. 2, p. 739, DESY Hamburg, 1988
24. D. Atwood, U. Baur, G. Couture, D. Zeppenfeld: CERN preprint TH 5213/88 (1988), DPF Summer Study Snowmass 1988, p. 264
25. M. Böhm, A. Rosado: Z. Phys. C – Particles and Fields 34 (1987) 117
26. U. Baur, J.J. van der Bij: In: Proceedings of the HERA Workshop. R.D. Peccei (ed.) Vol. 1, p. 495, DESY Hamburg, 1988; G.A. Schuler: Nucl. Phys. B299 (1988) 21; U. Baur, J.J. van der Bij: Nucl. Phys. B304 (1988) 451; M. Gluck, R.M. Godbole, E. Reya: Z. Phys. C – Particles and Fields 38 (1988) 441; ibid. Erratum 39 (1988) 590
27. J.J. van der Bij: Talk at the LHC Worksjop, DESY 11th June 1990; The third paper in [26]